

# Incommensurate antiferromagnetic fluctuations in the two-dimensional Hubbard model

H. C. Krah, S. Friederich, and C. Wetterich

*Institut für Theoretische Physik, Universität Heidelberg, Philosophenweg 16, D-69120 Heidelberg, Germany*

Commensurate and incommensurate antiferromagnetic fluctuations in the two-dimensional repulsive  $t - t'$ -Hubbard model are investigated using functional renormalization group equations. For a sufficient deviation from half filling we establish the existence of local incommensurate order below a pseudocritical temperature  $T_{pc}$ . Fluctuations not accounted for in the mean field approximation are important—they lower  $T_{pc}$  by a factor  $\approx 2.5$ .

PACS numbers: 71.10.Fd; 71.10.-w; 74.20.Rp

The two-dimensional Hubbard model [1, 2, 3] has attracted much interest in the past two decades because it is a candidate model for the  $\text{CuO}_2$ -planes in the high  $T_c$ -cuprates and may exhibit d-wave superconducting order [4, 5] at finite chemical potential. The model shows other interesting order structures such as incommensurate antiferromagnetism which appears close to half filling.

We focus on repulsive interactions  $U$  and not too large next-to-nearest neighbour hopping  $t'$ , where the model is an antiferromagnet at half filling. Not so far away from half-filling a more complicated form of antiferromagnetism, namely incommensurate antiferromagnetism is suggested by mean field computations and numerical studies for finite systems [6, 7, 8, 9, 10, 11, 12]. Incommensurate antiferromagnetism is related to the existence of spiral magnetic states which occur at large values of  $U$  [13, 14, 15]. Experimentally, incommensurate antiferromagnetism manifests itself in the peak structure of the magnetic structure factor which is accessible via neutron-scattering. It has been observed for a variety of high  $T_c$ -cuprates, for experimental and numerical results see [16, 17, 18, 19, 20, 21, 22].

In the temperature region where local incommensurate antiferromagnetic order supposedly sets in, the effective interaction between the electrons is large such that perturbative methods are not reliable. Collective fluctuations of electron-hole pairs in the antiferromagnetic channel play an important role. Since they are omitted in a mean field treatment one may doubt whether the mean field results for incommensurate antiferromagnetism are reliable. For these reasons we investigate the issue of incommensurate antiferromagnetism by a method that is intrinsically non-perturbative and includes effective collective bosonic fluctuations, namely the functional renormalization group for the “flowing action” (or “average action”)  $\Gamma_k$  [23, 24]. For this scale dependent effective action (or coarse grained free energy) the scale  $k$  indicates an infrared cutoff such that only fluctuations with momenta larger than  $k$  are effectively included. (Finally, one is interested in the limit  $k \rightarrow 0$ , where  $\Gamma_{k \rightarrow 0}$  equals the effective action—the generating functional of 1PI-correlation functions—including all fluctuations.) We will work in a version where the dominant collective bosonic fluctuations are represented by bosonic fields [25, 26]. Our model is equivalent to the purely fermionic Hubbard model from which it is derived by means of a Hubbard-Stratonovich transformation [27, 28]. (For functional renormalization group studies in a purely fermionic formulation see

[31, 32, 33, 34, 35].)

Our ansatz for the flowing action includes contributions for the electrons, for the bosons in both the antiferromagnetic and d-wave superconducting channels, and for interactions between fermions and bosons:

$$\Gamma_k[\chi] = \Gamma_{F,k}[\chi] + \Gamma_{\mathbf{a},k}[\chi] + \Gamma_{F\mathbf{a},k}[\chi] + \Gamma_{d,k}[\chi] + \Gamma_{Fd,k}[\chi]. \quad (1)$$

The collective field  $\chi = (\mathbf{a}, d, d^*, \psi, \psi^*)$  describes fermion fields  $\psi, \psi^*$ , the “antiferromagnetic boson field”  $\mathbf{a}$  and the complex field  $d$  a finite expectation value of which signals d-wave superconductivity. The fermionic kinetic term

$$\Gamma_{F,k} = \sum_Q \psi^\dagger(Q) P_F(Q) \psi(Q) \quad (2)$$

involves the inverse fermion propagator

$$P_F(Q) = Z_F(i\omega + \xi(\mathbf{q})), \quad (3)$$

where  $\xi(\mathbf{q}) = -\mu - 2t(\cos q_1 + \cos q_2) - 4t' \cos q_1 \cos q_2$  depends on the chemical potential  $\mu$  and the nearest and next-to-nearest neighbor hopping parameters  $t$  and  $t'$  of the Hubbard model. We employ a compact notation  $X = (\tau, \mathbf{x})$ ,  $Q = (\omega, \mathbf{q})$ ,

$$\begin{aligned} \sum_X &= \int_0^\beta d\tau \sum_{\mathbf{x}}, \quad \sum_Q = T \sum_{n=-\infty}^{\infty} \int_{-\pi}^{\pi} \frac{d^2 q}{(2\pi)^2}, \\ \delta(X - X') &= \delta(\tau - \tau') \delta_{\mathbf{x}, \mathbf{x}'}, \\ \delta(Q - Q') &= \beta \delta_{n, n'} (2\pi)^2 \delta^{(2)}(\mathbf{q} - \mathbf{q}'). \end{aligned} \quad (4)$$

where all components of  $X$  or  $Q$  are measured in units of the lattice distance  $a$  or  $a^{-1}$ . The discreteness of the lattice is reflected by the  $2\pi$ -periodicity of the momenta  $\mathbf{q}$ . A scale dependent fermionic wave function renormalization  $Z_F$  is included in Eq. (2).

The purely antiferromagnetic bosonic term is described by a kinetic term and a local effective potential

$$\Gamma_{a,k} = \frac{1}{2} \sum_Q \mathbf{a}^T(-Q) P_a(Q) \mathbf{a}(Q) + \sum_X U_{a,k}[\mathbf{a}], \quad (5)$$

where we employ a quartic effective potential  $U_{\mathbf{a}}$  for  $\mathbf{a}$ :

$$U_{\mathbf{a}}[\mathbf{a}] = \bar{m}_a^2 \alpha + \frac{1}{2} \bar{\lambda}_a \alpha^2, \quad (6)$$

with  $\alpha = \mathbf{a}^2/2$ . The kinetic term  $P_a$  involves the  $Q$ -dependent part of the inverse antiferromagnetic propagator and therefore contains the essential information about different kinds of magnetism. Our treatment of this term is discussed in detail below. Local antiferromagnetic order in domains of size  $k^{-1}$  is signalled by a minimum of  $\Gamma_{a,k}$  for  $\mathbf{a}(Q) \neq 0$ . For  $Q = 0$  this describes commensurate antiferromagnetism, while a minimum for non-vanishing  $\mathbf{q}$  in  $Q = (0, \mathbf{q})$  indicates incommensurate antiferromagnetism. A Yukawa-like interaction term couples the bosonic field to the fermions,

$$\Gamma_{F\mathbf{a},k} = -\bar{h}_a \sum_{K,Q,Q'} \delta(K + \Pi - Q + Q') \times \mathbf{a}(K) \cdot [\psi^\dagger(Q) \boldsymbol{\sigma} \psi(Q')], \quad (7)$$

where the momentum vector  $\Pi$  is given by  $\Pi = (0, \pi, \pi)$ .

The bosonic field  $d$  is associated to Cooper-pairs in the d-wave channel. It is described in more detail in [29, 30] where the exact form of  $\Gamma_{Fd}$  can be found. In this note we include the effect of d-wave fluctuations on the flow of the fermionic and “antiferromagnetic” part of  $\Gamma_k$ . We use  $\Gamma_{d,k} = \sum_Q d^*(Q) P_d(Q) d(Q) + \sum_X U_{d,k} [d, d^*]$  with  $U_d[d, d^*] = \bar{m}_d^2 \delta + \bar{\lambda}_d \delta^2/2$  where  $\delta = d^* d$ .

The dependence of the flowing action on the scale  $k$  is described by an exact flow equation [23]. Our ansatz (1) approximates the solutions to this functional differential equation. At the microscopic scale  $k = \Lambda$  the flowing action must be equivalent to the microscopic action of the Hubbard model. We therefore start the flow with “initial conditions”

$$\bar{m}_a^2|_\Lambda = U/3, \quad \bar{h}_a|_\Lambda = U/3, \quad \bar{\lambda}_a|_\Lambda = 0, \quad P_a(Q)|_\Lambda = 0, \\ \Gamma_{Fd}|_\Lambda = 0, \quad \Gamma_d|_\Lambda = d^* d, \quad Z_F|_\Lambda = 1. \quad (8)$$

At the microscopic scale  $\Lambda$ , the action for  $\mathbf{a}$  is Gaussian such that  $\mathbf{a}$  can be “integrated out” by solving its field equation as a functional of  $\psi$ . The d-boson decouples and becomes irrelevant. This demonstrates that  $\Gamma_\Lambda$  indeed coincides with the purely fermionic Hubbard model with repulsive coupling  $U > 0$ .

We still have to specify the truncation for the kinetic term of the  $\mathbf{a}$ -boson  $P_a(Q)$ . This is a central object of this paper, since incommensurate antiferromagnetic fluctuations will dominate if the minimum of  $P_a(0, \mathbf{q})$  occurs for nonzero  $\mathbf{q}$ . In order to gain some first information about the general shape of  $P_a$  we compute the mean field contribution from the fermionic loop

$$\Delta P_a(Q) = \sum_P \frac{\bar{h}_a^2}{P_F(Q + P + \Pi) P_F(P)} + (Q \rightarrow -Q). \quad (9)$$

The general features of this mean field contribution are used in order to motivate the form of the bosonic propagator in our truncation. We observe close to half filling two qualitatively different situations. At half filling and for sufficiently high temperatures also close to half filling there is a pronounced minimum at  $\mathbf{q} = 0$ , see Fig. 1 (a). However, away from half filling the picture is different for sufficiently low temperatures, see Fig. 1 (b). In the center at  $\mathbf{q} = 0$  there is a local maximum and there are four minima at positions

$$\mathbf{q}_{1,2} = (\pm \hat{q}, 0), \quad \mathbf{q}_{3,4} = (0, \pm \hat{q}), \quad (10)$$

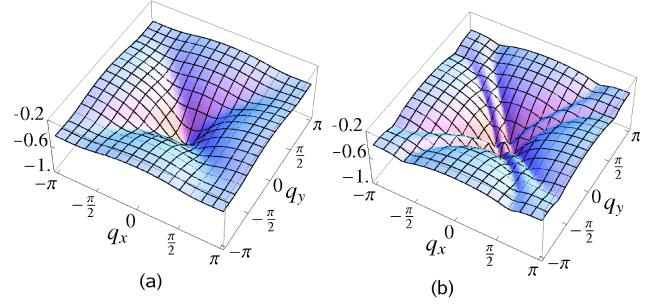


FIG. 1: Mean field kinetic term  $P_a(0, \mathbf{q})/t$  of the  $\mathbf{a}$ -boson as a function of space-like momenta for  $U/t = 3$  and  $t' = 0$ . In Figure (a)  $\mu = 0$  and  $T/t = 0.205$ , in Figure (b)  $\mu/t = -0.27$  and  $T/t = 0.0435$ . Both temperatures are mean field critical temperatures.

where  $\hat{q}$  is a function of  $T$ ,  $\mu$ , and  $t'$ . This is a manifestation of the dominance of *incommensurate* antiferromagnetic fluctuations.

Once the minimal value of the inverse bosonic propagator  $[P_a(0, \mathbf{q}) + \bar{m}_a^2]$  at zero frequency becomes smaller than zero, the minimum of the free energy can no longer occur for  $\langle \mathbf{a}(Q) \rangle = 0$ . One rather expects spontaneous symmetry breaking with a non-zero expectation value of  $\langle \mathbf{a} \rangle$ . As long as the minimum of  $P_a(0, \mathbf{q})$  is located at  $\mathbf{q} = 0$ , the order parameter  $\langle |\mathbf{a}| \rangle \sim \delta(\mathbf{q})$  indicates commensurate antiferromagnetism. However, for a minimum at  $\mathbf{q} = \mathbf{q}_j \neq 0$  the incommensurate antiferromagnetic order breaks further lattice symmetries. One of the pairs of minima (10) is selected and the symmetry of rotations by  $\pi/2$  around  $\mathbf{q} = 0$  in momentum space is spontaneously broken. The spins change sign between neighboring lattice sites only in one direction, the  $x$ -direction say, whereas in the orthogonal direction the periodicity corresponds to some momentum  $\pi \pm \hat{q}$ . The state with  $\langle \mathbf{a} \rangle = 0$  becomes unstable when  $(P_a)_{\min} = -\bar{m}_a^2$ . In case of a second order phase transition this occurs for the mean field critical temperature  $T = T_{MFC}$ . Figures 1 (a) and (b) correspond to mean field critical temperatures. Note that the system selects one of the *pairs*  $\mathbf{q}_{1,2}$  or  $\mathbf{q}_{3,4}$  since  $\mathbf{a}(X)$  is a real field. Therefore the system remains symmetric with respect to reflection about the axes.

We are interested in whether incommensurate antiferromagnetism persists if bosonic fluctuations are included. Taking into account bosonic fluctuations, the critical temperature vanishes in the infinite volume limit due to the Mermin-Wagner theorem. The destruction of local order by the long range fluctuations of the Goldstone bosons (antiferromagnetic spin waves) is only a logarithmic effect, however. For a probe of finite macroscopic size antiferromagnetic order can be observed and the critical temperature is nonzero [26]. Here the effective critical temperature  $T_c$  is defined such that for  $T < T_c$  the typical size of ordered domains exceeds the macroscopic size of the probe  $l$ . In other words,  $\langle \mathbf{a}(k) \rangle$  differs from zero for  $k_{ph} = l^{-1}$  if  $T < T_c$ , while for  $T > T_c$  one has  $\langle \mathbf{a}(k) \rangle = 0$ .

In this note we only study the pseudo critical temperature  $T_{pc}$  which marks the onset of local ordering corresponding to

a minimum of the flowing action  $\Gamma_k$  for  $\mathbf{a}(0, \mathbf{q})$ . Above this temperature,  $\langle |\mathbf{a}| \rangle = 0$  holds on all scales of the renormalization flow. For  $T < T_{pc}$  local order sets in for  $k = k_c > 0$ . In case of incommensurate antiferromagnetism we expect the formation of domain walls between regions where  $\hat{\mathbf{q}}$  points in the  $x$ - or  $y$ -direction. This contrasts with commensurate antiferromagnetism where only a continuous symmetry is broken for  $\mathbf{a} \neq 0$ . For  $k < k_c$  the flow should then be continued in a regime with nonzero  $\mathbf{a}$  in order to account properly for the Goldstone boson fluctuations. This has been investigated for the commensurate case in [26], but is not yet implemented for the incommensurate case in the present note. We note that  $T_{pc}$  is the equivalent of the mean field critical temperature. For  $T_c < T < T_{pc}$  the electron propagator does not exhibit a true gap, but it is suppressed for momenta corresponding to the inverse of length scales for which local order is present.

Inspired by the shape of  $P_a$  in the mean field approximation we approximate the kinetic term for the antiferromagnetic boson by

$$P_{a,k}(Q) = Z_a \omega^2 + A_a F(\mathbf{q}), \quad (11)$$

where for the case of commensurate antiferromagnetism we choose for  $F(\mathbf{q})$

$$F_c(\mathbf{q}) = \frac{D^2 [\mathbf{q}]^2}{D^2 + [\mathbf{q}]^2}. \quad (12)$$

Here  $[\mathbf{q}]^2$  is defined as  $[\mathbf{q}]^2 = q_1^2 + q_2^2$  for  $q_i \in [-\pi, \pi]$  and continued periodically otherwise. For small  $\mathbf{q}^2$  the quadratic approximation  $P_a = A_a \mathbf{q}^2$  describes a linear dispersion relation for the composite bosonic field,  $\omega = \sqrt{A_a/Z_a} |\mathbf{q}|$ , while for  $\mathbf{q}$  near the boundary of the Brillouin zone the momentum dependence of  $P_a$  ‘levels off’ as in Figs. 1 (a), (b). For a suitable choice of  $A_a$  and  $D$  the shape of the mean field result for  $P_a$  is well reproduced. Of course, due to the important contributions of bosonic fluctuations beyond mean field theory, the actual values of  $A_a$  and  $D$  will differ substantially from the mean field values.

Within the functional renormalization group approach, we describe the scale dependence of the bosonic kinetic term by flow equations for the parameters  $A_a$  and  $D$ . For these purposes we define the gradient coefficient  $A_a$  by

$$A_a = \frac{1}{2} \frac{\partial^2}{\partial l^2} P_a(0, l, 0) \Big|_{l=\hat{q}} \quad (13)$$

with  $\hat{q} = 0$  in the commensurate case. The shape coefficient  $D$  is computed as

$$D^2 = \frac{1}{A_a} (P_a(0, \pi, \pi) - P_a(0, \hat{q}, 0)). \quad (14)$$

The flow equations for  $A_a$  and  $D$  can be extracted by inserting our truncation in the exact flow equations for the kinetic term (11).

During the renormalization flow the gradient coefficient  $A_a$  first increases, starting from  $A_a = 0$  at the scale  $\Lambda$ . At half filling and in the proximity of half filling for sufficiently high

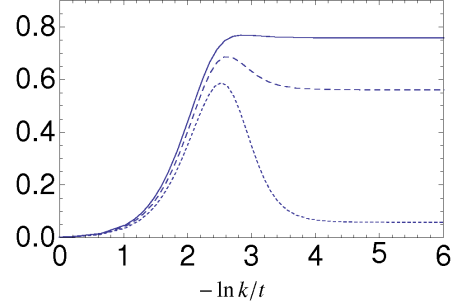


FIG. 2: Flow of the gradient coefficient  $A_{a,k}$  at  $\mu/t = -0.12$  in the temperature regime where we have commensurate antiferromagnetism. The solid line corresponds to  $T/t = 0.08$ , the long-dashed line to  $T/t = 0.07$ , and the short-dashed line to  $T/t = 0.058$ .

temperatures,  $A_a$  either increases monotonically or at least remains larger than zero on all scales  $k < \Lambda$ , see Fig. 2. The minimum of  $P_a$  occurs for  $\mathbf{q} = 0$  and commensurate antiferromagnetic fluctuations dominate.

However, for low enough temperatures and at sufficient distance from half-filling,  $A_a$  becomes zero on a certain scale. If we continued to evaluate  $A_a$  for  $\mathbf{q} = 0$  it would decrease to negative values for lower scales. This situation corresponds to the case of incommensurate antiferromagnetism. The ansatz for the function  $F(\mathbf{q})$  given in Eq. (12) is no longer suitable. One has to allow for the existence of minima of  $P_{a,k}(0, \mathbf{q})$  at nonzero  $\mathbf{q} \neq 0$ . The ansatz (11) for the inverse bosonic propagator employs now for  $F(\mathbf{q})$

$$F_i(\mathbf{q}, \hat{q}) = \frac{D^2 \tilde{F}(\mathbf{q}, \hat{q})}{D^2 + \tilde{F}(\mathbf{q}, \hat{q})}. \quad (15)$$

The quadratic momentum dependence of the numerator in (12) is replaced by an expression which is quartic in momentum and explicitly includes the incommensurability  $\hat{q}$ :

$$\tilde{F}(\mathbf{q}, \hat{q}) = \frac{1}{4\hat{q}^2} ((\hat{q}^2 - [\mathbf{q}]^2)^2 + 4[q_x]^2 [q_y]^2). \quad (16)$$

The first term in  $\tilde{F}$  vanishes for  $[\mathbf{q}]^2 = \hat{q}^2$  and suppresses the propagator for  $[\mathbf{q}]^2 \neq \hat{q}^2$ . The second term favours the minima (10) as compared to a situation where rotation-symmetry in the  $q_x - q_y$ -plane is preserved. The prefactor is determined by Eq. (13). For  $\hat{q} \rightarrow 0$  one has  $A_a \sim \hat{q}^2$  such that  $P_a$  becomes quartic in  $\mathbf{q}$ . We compare in Fig. 3 the kinetic term  $P_a(0, \mathbf{q})$  in mean field theory with the approximation from our ansatz.

In Fig. 4, a typical flow for  $A_a$  and  $\hat{q}$  in the incommensurate regime is displayed. For scales below the scale where  $A_a$  becomes zero,  $\hat{q}$  increases to a finite value and  $P_a(0, \mathbf{q})$  has four degenerate minima at positions given by Eq. (10). The solution  $\hat{q}$  of Eq. (20) at the end of the flow corresponds to the position of the minimum, e.g., at the positive  $q_x$ -axis. We next specify the flow in more detail.

The regulator function  $R_k^a(Q)$  for the antiferromagnetic fluctuations should be adapted in order to allow for the dominance of incommensurate antiferromagnetism. We employ,

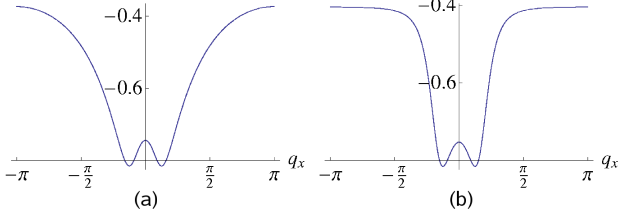


FIG. 3: In (a) the mean field approximation for the kinetic term  $P_a(0, q_x, 0)/t$  is shown as a function of the  $x$ -component of spatial momenta. Parameters are  $U/t = 3$ ,  $\mu/t = -0.35$ ,  $t' = 0$  and  $T/t = 0.1$ . In (b) the approximation given by Eq. (16) is displayed for  $k = 0$ . Minima occur at positions  $\mathbf{q}_{1,2} = (\pm\hat{q}, 0) = (\pm 0.393, 0)$ .

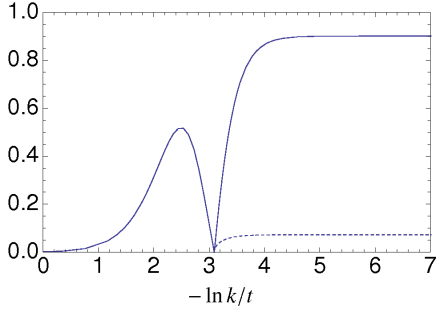


FIG. 4: Flow of the gradient coefficient  $A_{a,k}$  and the incommensurability  $\hat{q}$  at  $\mu/t = -0.12$  and  $T/t = 0.05$ , where incommensurate antiferromagnetism dominates. The solid line shows  $A_a$  decreasing to zero at  $-\ln k/t = 3.09$  and increasing again when the incommensurability  $\hat{q}$  (short-dashed line) sets in.

similarly for the commensurate and incommensurate case,

$$R_k^a(Q) = A_a \cdot (k^2 - F_{c,i}(\mathbf{q}, \hat{q}))\Theta(k^2 - F_{c,i}(\mathbf{q}, \hat{q})), \quad (17)$$

respectively. This generalizes the cutoff chosen in [30].

The flow equation for the gradient coefficient is obtained by taking appropriate derivatives in one of the minima

$$\begin{aligned} \partial_k A_a &= \sum_Q \bar{h}_a^2 \tilde{\partial}_k \frac{\partial^2}{\partial l^2} \frac{1}{P_F^k(Q) P_F^k(K + Q + \Pi)} \Big|_{l=\hat{q}} \\ &+ \sum_Q \bar{h}_a^2 (\partial_k \hat{q}) \frac{\partial^3}{\partial l^3} \frac{1}{P_F^k(Q) P_F^k(K + Q + \Pi)} \Big|_{l=\hat{q}}, \end{aligned} \quad (18)$$

where  $K = (0, l, 0)$ . We have defined  $P_{F,k}(Q) = P_F(Q) + R_k^F(Q)$ , with fermion cutoff  $R_k^F$  chosen as in [30]. The first term in (18) results from the change of the infrared cutoff in the fluctuations. The symbol  $\tilde{\partial}_k$  means a formal derivative with respect to the cutoff function  $R_k^F$ . The second term in (18) reflects the shift of the location of the minimum of  $P_a$  at  $(\hat{q}, 0)$  and is absent if commensurate fluctuations dominate,  $\hat{q} = 0$ .

A flow equation for the position of the minima  $\hat{q}$  is derived from the condition

$$\frac{\partial}{\partial q_x} P_{a,k}(0, \mathbf{q}) \Big|_{\mathbf{q}=(\hat{q},0)} = 0. \quad (19)$$

Taking the scale derivative of this equation one obtains the flow equation:

$$\begin{aligned} (\partial_k \hat{q}) \frac{\partial^2}{\partial q_x^2} P_{a,k}(0, \mathbf{q}) \Big|_{\mathbf{q}=(\hat{q},0)} + \frac{d}{dk} \Big|_{\hat{q}} \frac{\partial}{\partial q_x} P_{a,k}(0, \mathbf{q}) \Big|_{\mathbf{q}=(\hat{q},0)} \\ = (\partial_k \hat{q}) 2A_a + \frac{d}{dk} \Big|_{\hat{q}} \frac{\partial}{\partial q_x} P_{a,k}(0, \mathbf{q}) \Big|_{\mathbf{q}=(\hat{q},0)} = 0. \end{aligned} \quad (20)$$

Flow equations for the other running couplings  $Z_F, \bar{m}_a^2, \bar{\lambda}_a, \bar{h}_a, \bar{m}_d^2, \bar{\lambda}_d, \bar{h}_d, D$  are not given explicitly here, see [30].

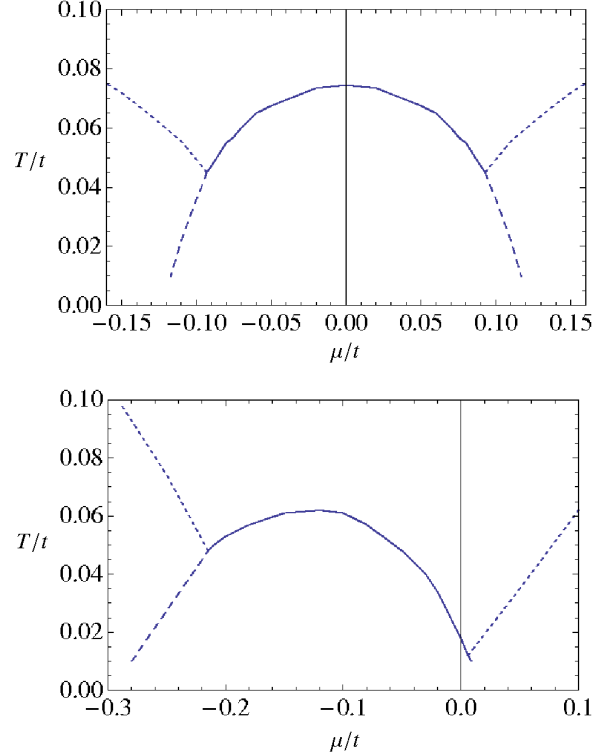


FIG. 5: Pseudo-critical temperature  $T_{pc}/t$  as a function of  $\mu/t$ , given by the solid (commensurate) and dashed (incommensurate) lines. Results are displayed for  $U/t = 3$ ,  $t' = 0$  (upper panel) and  $t'/t = -0.05$  (lower panel).

We now turn to our results. An overview of the occurrence of incommensurate antiferromagnetism is given in Fig. 5, showing pseudo-critical temperatures  $T_{pc}$  for the different kinds of antiferromagnetic order in the presence of vanishing (upper panel) and nonvanishing (lower panel) next-to-nearest neighbor hopping  $t'$ . The solid line signals the onset of local commensurate, the long-dashed line the onset of local incommensurate antiferromagnetic order. Below the short-dashed line there is no local magnetic order but incommensurate fluctuations dominate. Below the point where the short-dashed line terminates at low temperatures, numerical solutions to the flow equations, as we have implemented them numerically, are no longer reliable. For both vanishing and non-vanishing  $t'$ , one observes commensurate antiferromagnetism for a certain range of chemical potential  $\mu$ , while for smaller and larger

values of  $\mu$  incommensurate fluctuations begin to dominate. For finite  $t'$ , however, the pseudo-critical curve is no longer the same for positive and negative  $\mu$  but, for negative  $t'$ , is shifted to more negative values of  $\mu$ .

The pseudo-critical temperature is found to be substantially lower than according to the mean field computation. For  $U = 3t$ ,  $t' = 0$  and  $\mu = 0$ , for example, the mean-field computation gives  $T_{MFc}/t = 0.205$ , while we find  $T_{pc}/t = 0.0745$  when one takes into account bosonic fluctuations. By reducing the interaction, the shape of the pseudo-critical curve remains the same but local order emerges only at lower temperatures.

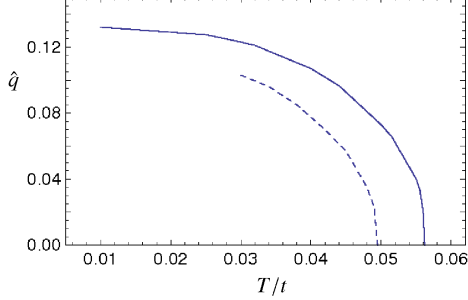


FIG. 6: Incommensurability  $\hat{q}$  as a function of  $T$  for  $U/t = 3$ ,  $t' = 0$  and  $\mu/t = -0.12$  (solid line) and  $\mu/t = -0.105$  (dashed line).

With decreasing temperature the tendency towards incommensurate fluctuations is increased, which can be demonstrated by studying the dependence of  $\hat{q}$  on  $T$  at fixed chemical potential. It is shown for  $\mu/t = -0.105$  and  $\mu/t = -0.12$  in Fig. 6. For large enough temperatures one has  $\hat{q} = 0$ , while below some  $\mu$ -dependent temperature incommensurate antiferromagnetism sets in. The temperature where this happens is indicated by the short-dashed line in Fig. 5 (upper panel). For smaller  $T$  the value of  $\hat{q}$  increases, the final point of the  $\mu/t = -0.105$ -curve at low temperature corresponds to the long-dashed line in Fig. 5.

A dominance of incommensurate antiferromagnetic fluctuations can be observed in the momentum dependence of the magnetic susceptibility and the bosonic occupation number. The susceptibility is given by the bosonic propagator at zero frequency  $P_a^{-1}(0, \mathbf{q})$ , while the occupation number is obtained by an additional sum over bosonic Matsubara frequencies,  $n_a(\mathbf{q}) = T \sum_{\omega_B} (P_a(\omega_B, \mathbf{q}))^{-1}$ . Fig. 7 shows that for parameters where the bosonic mass is small, here  $\bar{m}_a^2/U \approx 10^{-2}$ , and thus close to the onset of local incommensurate order, both the magnetic susceptibility and the bosonic occupation number are peaked at  $q_x = \pm\hat{q}$ , signalling that incommensurate fluctuations strongly dominate. The situation is completely analogous for the  $q_y$ -dependence of the susceptibility at  $q_x = 0$ , whereas both quantities do not have such a pronounced peak structure along the Brillouin zone diagonal.

A mean field analysis is probably the simplest way to get a glimpse at those regions of the phase diagram which exhibit either commensurate or incommensurate antiferromagnetic order. A more extensive treatment of the commensurate case with nonzero next-to-nearest neighbor hopping  $t'$  can be

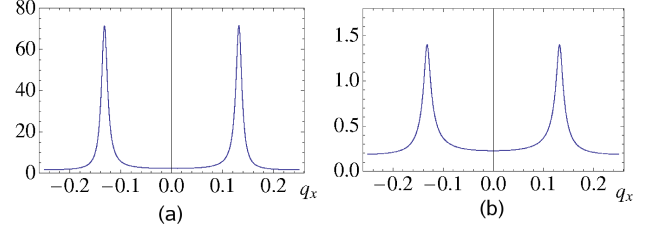


FIG. 7: Fig. (a) shows the spin susceptibility  $(P_a(0, q_x, 0)/t)^{-1}$  and Fig. (b) the bosonic occupation number  $n_a(q_x, 0)$  for  $\mu/t = -0.12$ ,  $T/t = 0.01$ ,  $U/t = 3$  and  $t' = 0$ . Both curves are given as a function of spatial momentum in  $x$ -direction. A peak at  $q_x = 0$  would signal the dominance of commensurate antiferromagnetism. The actual peaks, located at  $\hat{q} = \pm 0.132$ , indicate incommensurate antiferromagnetism.

found in [36]. For a system in the Néel state the periodicity is changed resulting in a novel “magnetic” Brillouin zone whose boundaries are given by the lines between the  $(\pm\pi, 0)$  and  $(0, \pm\pi)$  points. Correspondingly, the mean field dispersion relation for a nonzero gap parameter  $A = \bar{h}_a \langle |\mathbf{a}| \rangle$  has two branches

$$E_{\pm}(\mathbf{p}) = \frac{1}{2} \left( \xi(\mathbf{p}) + \xi(\mathbf{p} + \boldsymbol{\pi}) \pm \sqrt{(\xi(\mathbf{p}) - \xi(\mathbf{p} + \boldsymbol{\pi}))^2 + 4A^2} \right)$$

which, for finite  $t'$ , lead to an interestingly structured effective Fermi surface enclosing hole pockets around  $(\pm\pi/2, \pm\pi/2)$  and electron pockets around  $(\pm\pi, 0)$  and  $(0, \pm\pi)$ , see the example drawn in Fig. 8 (a), for further details see e. g. [36].

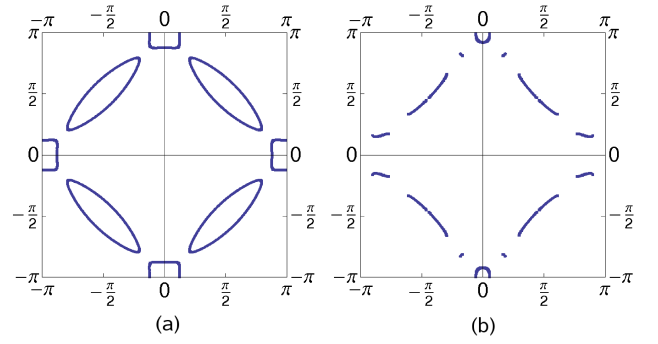


FIG. 8: Effective Fermi surfaces for  $\mu/t = -0.6$ ,  $t'/t = -0.2$  and gap parameter  $A/t = 0.1$ . Fig. (a) shows the commensurate case  $\hat{q} = 0$  where the Fermi surface exhibits hole- and particle pockets at the magnetic Brillouin zone boundary. In Fig. (b), the remainders of the effective Fermi surface are shown for a nonzero incommensurability  $\hat{q} = 0.3$  along the  $x$ -axis.

In the presence of a nonzero expectation value  $\langle \mathbf{a}(\hat{\mathbf{q}}) \rangle$  with  $\hat{\mathbf{q}} \neq 0$ , the inverse of the fermionic mean field propagator at zero frequency has contributions from Eqs. (3)(with  $Z_F = 1$ ) and (7) and is given by

$$P_F(\mathbf{q}, \mathbf{q}') = \xi(\mathbf{q})\delta(\mathbf{q} - \mathbf{q}') - \frac{\mathbf{A} \cdot \boldsymbol{\sigma}}{\sqrt{2}} (\delta(\mathbf{q} - \mathbf{q}' - \boldsymbol{\pi} + \hat{\mathbf{q}}) + \delta(\mathbf{q} - \mathbf{q}' - \boldsymbol{\pi} - \hat{\mathbf{q}})) \quad (21)$$



with  $\hat{\mathbf{q}} = \mathbf{q}_{1,2}$  or  $\hat{\mathbf{q}} = \mathbf{q}_{3,4}$  as defined in Eq. (10). The analogue of the Fermi surface corresponds to the zero eigenvalues of  $P_F$ . However, the corresponding eigenmodes are no longer momentum eigenstates. Nevertheless, if the gap parameter  $A = |\mathbf{A}|$  is nonzero but small, many eigenvalues of  $P_F(\mathbf{q}, \mathbf{q}')$  have most of their support each at a single momentum  $\mathbf{p}$ . This concerns all those momenta  $\mathbf{p}$  for which the condition

$$A \ll |\xi(\mathbf{p} + \boldsymbol{\pi} + \hat{\mathbf{q}})|, |\xi(\mathbf{p} + \boldsymbol{\pi} - \hat{\mathbf{q}})| \quad (22)$$

is fulfilled. With respect to these momenta the equation

$$\xi(\mathbf{p}) - \frac{A^2}{2} \left( \frac{1}{\xi(\mathbf{p} + \boldsymbol{\pi} + \hat{\mathbf{q}})} + \frac{1}{\xi(\mathbf{p} + \boldsymbol{\pi} - \hat{\mathbf{q}})} \right) = 0 \quad (23)$$

defines an effective Fermi surface which is obtained by (approximately) diagonalizing  $P_F(\mathbf{q}, \mathbf{q}')$  for small  $A$ . For large enough  $A$  the effective Fermi surface vanishes completely because the number of solutions to Eq. (23) that satisfy the condition (22) rapidly goes down. In Fig. 8 (b) the effective Fermi

surface is shown for the incommensurate case with an order parameter  $\langle \mathbf{a}(\hat{\mathbf{q}}) \rangle$  where  $\hat{\mathbf{q}} = \mathbf{q}_{1,2}$ , i.e. the incommensurability is along the  $x$ -axis. The symmetry of rotations by  $\pi/2$  is manifestly broken.

To summarize, we have shown that incommensurate anti-ferromagnetic order in the two-dimensional Hubbard model persists if bosonic fluctuations are taken into account. This phenomenon occurs at least in the form of local order for temperatures smaller than the pseudocritical temperature shown in Fig. 5. We speculate that for  $T \rightarrow 0$  the size of the incommensurate domains grows beyond the size of typical macroscopic probes, but this remains to be shown. If magnetic fluctuations play a role in the generation of d-wave superconducting order, the effect of incommensurability has to be taken into account.

**Acknowledgments:** HCK acknowledges financial support by the DFG research unit FOR 723 under the contract WE 1056/9-1. SF acknowledges support by the Studienstiftung des Deutschen Volkes.

- 
- [1] J. Hubbard, Proc. R. Soc. London, Ser. A **276**, 276 (1963).
  - [2] J. Kanamori, Prog. Theor. Phys. **30**, 275 (1963).
  - [3] M. C. Gutzwiller, Phys. Rev. Lett. **10**, 159 (1963).
  - [4] P. W. Anderson, Science **235**, 1196 (1987).
  - [5] D. J. Scalapino, Physics Reports **250**, 329 (1995).
  - [6] H. J. Schulz, Phys. Rev. Lett. **64**, 1445 (1990).
  - [7] P. Benard, L. Chen and A.-M. S. Tremblay, Phys. Rev. B **47**, 589 (1993).
  - [8] A. V. Chubukov and K. A. Musaelian Phys. Rev. B **51**, 12605 (1995).
  - [9] P. Mancini, D. Villani and H. Matsumoto, Phys. Rev. B **57**, 6145 (1998).
  - [10] A. Moreo, D. J. Scalapino, R. L. Sugar and S. R. White, Phys. Rev. B **41**, 2313 (1990).
  - [11] N. Bulut, D. Hone, D. J. Scalapino and N. Bickers, Phys. Rev. Lett. **64**, 2723 (1990).
  - [12] H. Kaga and M. Cyrot, Phys. Rev. B **58**, 12267 (1998).
  - [13] S. Sarker, C. Jayaprakash, H.R. Krishnamurthy and W. Wenzel, Phys. Rev. B **43**, 8775 (1991).
  - [14] C. Zhou and H. J. Schulz, Phys. Rev. B **52**, 11557 (1995).
  - [15] C. Brügger, C. P. Hofmann, F. Kämpfer, M. Peper and U.-J. Wiese, Phys. Rev. B **52**, 11557 (1995).
  - [16] R. J. Birgeneau *et al.*, Phys. Rev. B **39**, 2868 (1989).
  - [17] S.-W. Cheong *et al.*, Phys. Rev. Lett. **67**, 1791 (1991).
  - [18] B. J. Sternlieb *et al.*, Phys. Rev. B **50**, 12915 (1994).
  - [19] F. Yuan *et al.*, Phys. Rev. B **64**, 224505 (2001).
  - [20] J. Lorenzana and G. Seibold, Phys. Rev. Lett. **89**, 136401 (2002).
  - [21] M. Fujita *et al.*, Phys. Rev. B **70**, 104517 (2004).
  - [22] G. Seibold and J. Lorenzana, Phys. Rev. Lett. **94**, 107006 (2005).
  - [23] C. Wetterich, Phys. Lett. B **301**, 90 (1993).
  - [24] J. Berges, N. Tetradis and C. Wetterich, Phys. Rep. **363**, 223 (2002).
  - [25] T. Baier, E. Bick and C. Wetterich, Phys. Rev. B **70**, 125111 (2004).
  - [26] T. Baier, E. Bick and C. Wetterich, Phys. Lett. B **605**, 144 (2005).
  - [27] J. Hubbard, Phys. Rev. Lett. **3**, 77 (1959).
  - [28] R. L. Stratonovich, Soviet. Phys. Doklady **2**, 416 (1958).
  - [29] H. C. Krahle and C. Wetterich, Phys. Lett. A **367**, 263 (2007).
  - [30] H. C. Krahle, J. A. Müller and C. Wetterich, arXiv.0801.1773v1[cond-mat.str-el], accepted for publication in Phys. Rev. B (2009).
  - [31] D. Zanchi and H. J. Schulz, Z.Phys. **B103**, 339 (1997).
  - [32] C. J. Halboth and W. Metzner, Phys. Rev. Lett. **85**, 5162 (2000).
  - [33] M. Salmhofer and C. Honerkamp, Prog. Theor. Phys. **105**, 1 (2001).
  - [34] C. Honerkamp, M. Salmhofer, N. Furukawa and T. M. Rice, Phys. Rev. B **63**, 035109 (2001).
  - [35] C. Honerkamp and M. Salmhofer, Phys. Rev. Lett. **87**, 187004 (2001).
  - [36] J. Reiss, D. Rohe and W. Metzner, Phys. Rev. B **75**, 075110 (2007).